Science Press

ARTICLE

Spheroidization of TC4 (Ti6Al4V) Alloy Powders by Radio Frequency Plasma Processing

Zhao Chong,   Ma Chaoyang,   Wen Zicheng,   Cao Yongge,   Ma Ran,   Yuan Xuanyi

Key Laboratory of Opto-electronic Functional Materials & Micro-nano Devices of Beijing, Renmin University of China, Beijing 100872, China

Abstract: Highly spherical TC4(Ti-6Al-4V) powders were produced by a radio frequency plasma system. The influential parameters, namely position of the inlet nozzle, plasma plate power, chamber pressure, particle size distribution of raw materials, the feeding rate and the flow rate of the carrier gas were changed solo and the spheroidization ratio was counted with the help of SEM images. The phase structure and morphology of the powders were investigated by XRD and SEM. The results show that the observation of the surface and cross section of the spherical particle indicates that the particles are dense with a relatively smooth surface. Fluidity and bulk density are both improved to be suitable for practical application. Spheroidization ratio as high as 99% has been reached when the position of the inlet nozzle is 12.5 cm, the chamber pressure is 101.36 kPa, the powder feeding rate is 1.742 g/min, the plasma plate power is 27.2 kW and the particle size distribution of raw particles is around 38~63 μm.

Key words: spheroidization; Ti6Al4V powders; RF induction plasma

Ti6Al4V (TC4) alloy is the most popular two phase titanium ($\alpha+\beta$) alloy as its total production is about half of all titanium alloys. TC4 alloy has great mechanical properties. In general, Ti6Al4V alloy has high specific strength, low density, better corrosion-resistance, high toughness, superior weldability and excellent bio-compatibility; thus this kind of titanium alloy has a wide range of industrial applications, especially for aviation, aerospace, and medical engineering[1-3].

Nowadays, 3D printing is one of the developments in rapid prototyping for producing spare parts for the airplane, artificial skeleton and other industrial sectors [4]. TC4, as one of widely used raw materials in industry is also a hot material for 3D printing. 3D printing asks for high fluidity of the materials and spheroidization procedure is a good approach to improve the fluidity. Compared with conventional processes, a radio frequency plasma spheroidization system has many advantages such as no pollution from electrode compared with plasma rotation electrode process and synthesis of nano-particles compared with an atomization method. Besides, RF induction plasma system has a high temperature flame (3000~10000K) and a rapidly cooling system (~10^6 K/s) so it

is perfect for refractory materials and producing spherical and uniform particles[5,6].

In this work, highly flowable and spherical particles of Ti6Al4V alloy have been produced by RF induction plasma system. The phase formation of powders through different processing process was detected by XRD, and morphologies of surfaces and cross-section of particles were investigated by means of SEM. The influential parameters have been changed sololy and the spheroidization ratio has been investigated.

1 Experiment

In this procedure, we used the SY119-30kW induction plasma system (Fig.1, Model PL-35 TEKNA Plasma Systems Inc., Canada) for the spheroidization process. We first sent the raw powders (TC4, $d \leq 45$ μm, Western BaoDe Technologies Co. Ltd, China) to the induction-plasma torch with a vibrating screw feeder (Model PFV 100-VM, TEKNA Plasma Systems Inc., Canada). The elementary composition of raw powders is listed in Table 1. Then the powders were heated with a really high temperature in the plasma plume and totally melted quickly. When the particles were flying out of the plasma
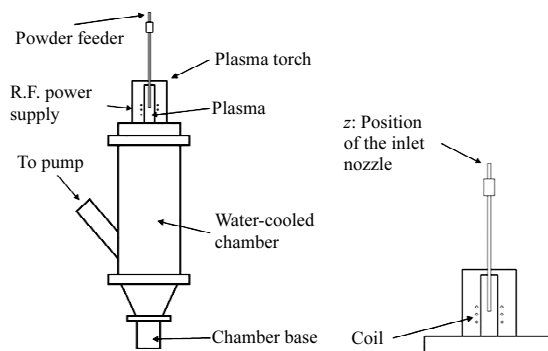
Fig.1   Schematic illustration of SY119-30 kW induction plasma system and the plasma torch

Table 1   Elementary composition of raw material TC4 alloy powders (wt%)

C	0.587
O	0.490
H	0.059
N	0.033
Fe	0.145
Al	5.750
V	3.750
Si	0.030

plume, they were cooled down rapidly with the high temperature gradient in the chamber. And because of the surface tension, the raw particles with irregular shape will turn to spherical ones. After a while, we can collect them in the chamber base.

In this work, we changed some processing parameters to investigate the spheroidization ratio. Temperature gradient of thermal plasma and dwell time for melting particles are two fundamental contributory factors. During the experiment, we can change the position of the inlet nozzle, plasma plate power and the type of the gas to obtain different temperature distribution. Besides, we can adjust the powder feeding rate, chamber pressure as well as the flow rate of carrier gas and sheath gas to change the dwell time for melting. As for the gas, argon is always a good choice for the carrier gas, central gas and sheath gas. To improve the spheroidization ratio, we tried to use hydrogen or nitrogen as the sheath gas due to their higher thermal conductivity[7]. The higher thermal conductivity of the plasma gas will lead to a higher heat-transfer efficiency so that the powders will melt faster and more sufficiently. In addition, because hydrogen and nitrogen are both diatomic molecules, the Ar-H_2 and the Ar-N_2 thermal plasma will have a higher enthalpy which makes the plasma have a higher temperature[8]. But in this experiment, we only chose high pure argon as the thermal plasma gas because titanium alloy will react with hydrogen or nitrogen to create $TiH_{1.5}$ (PDF#78-2216) or $TiN_{0.76}$ (PDF#87-0626).

The phase identification of raw materials (TC4 alloy powders) and the plasma spheroidized powders were carried out by X-ray diffraction (XRD, Bruker AXS, D8 ADVANCE A25-X1-1A32C4B, Germany). Morphologies of the raw Ti6Al4V powders and the spherical powders were observed by scanning electron microscopy (SEM, FEI, NOVA, NANOSEM, 450). The internal microstructure of spherical particles was observed by a 3-in-1 multi-beam ion microscope (Orion Nano Fab, Carl Zeiss Co., USA). The particle size distribution (PSD) of raw materials and spheroidized powders was evaluated with a laser particle size analyser (Winner 2000, Jinan Winner Particle Instruments Joint Stock Co. Ltd. China). Fluidity of the powders was investigated by the Holzer flow meter (HYL-102 Dandong Haoyu Technology Co. Ltd., China) and the bulk density was measured by bulk density meter (HYL-102 Dandong Haoyu Technology Co. Ltd, China).

After the spheroidization experiment, we counted the spheroidization ratio defined by the formula as follows:

$$\eta_s = \frac{B}{A} \times 100\%$$

where η_S, A and B are the spheroidization ratio, the amount of the spherical particles and the total number of the particles, respectively. For the sake of the accuracy, we chose three images of every sample and each image has more than 200 particles.

2   Results and Discussion

2.1   XRD analysis

Fig.2 shows the XRD patterns of all the samples before and after plasma treatment. The XRD pattern (in blue) of raw materials accords with the characteristic peaks of Ti (PDF# 44-1294), just like the bottom red columns index. The other three XRD patterns exhibit that, under different sheath gases (H_2, N_2), the spheroidized powders show some impurity peaks, while that with argon as the sheath gas does not. For XRD pattern in green (Ar-H_2), the impurity peaks match well with $TiH_{1.5}$ (PDF#78-2216), meaning that raw materials react with H_2 as we supposed to. Likewise, the XRD pattern in pink (Ar-N_2) prove that raw materials react with N_2 to produce $TiN_{0.76}$ (PDF#87-0626). In case of XRD pattern in wine (Ar-Ar), high pure argon was used as sheath gas, central gas and carrier gas, and the spheroidized powders keep the same XRD phase with raw materials.

2.2   Morphologies

Fig.3a shows the SEM image of TC4 alloy raw materials in irregular flake shape. While, the corresponding spheroidized powders are all spherical, as shown in Fig.3b. The internal microstructure of spheroidized TC4 alloy particles was investigated with a 3-in-1 multibeam ion microscope. First, a focused ion beam (FIB) was conducted to cut a chosen spherical particle into a hemispherical one. Then, the helium ion beam was used to observe the cross section. Because the incident ion beam has a small tilt angle, the fitted circle does
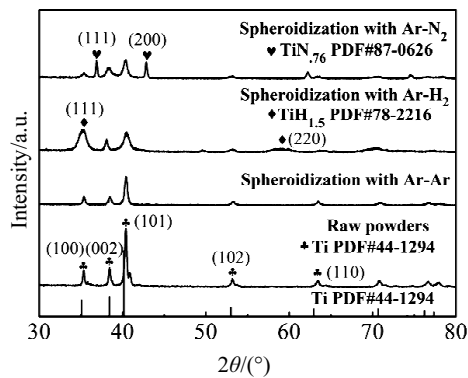
Fig.2   XRD patterns of powders before and after spheroidization with different sheath gas (27.2 kW, *v*=1.742 g/min, *p*=101.36 kPa, *z*=12.5 cm)

not match the hemispherical section well. The diameter of the spherical particle in Fig.3c was evaluated to be about 56.6 μm. The surface microstructure of the randomly chosen particle in Fig.3d is rough with shallow trenches. When the powders are flying out of the plasma plume, they will go through a steep temperature gradient and be cooled down at a high rate which will change the surface structure and allow the trenches to come into being[9].

One advantage of the spheroidizing process is that the diameters of the spheroidized particles can be controlled. Fig.4 shows that the size of the spheroidized powders has little

difference with the raw material powders, indicating that once the size of raw materials is controlled, the diameter of spheroidized powders is also fixed.

2.3   Contributory factors of spheroidization ratio

2.3.1   Power plate power

With a higher thermal plasma temperature, the powders will absorb more heat and melt more fully. In this procedure, plasma plate power directly influences the temperature gradient as well as the heat energy of the plasma[10]. We chose three levels of power as shown in Table 2. Comparing the spheroidization ratio of experiment No.2, No.3 and No.8 in Table 2, one can discover that the higher the plasma plate power is selected, the better the spheroidization ratio will be. And the trend is so clear with a nearly 20% increase of the spheroidization ratio when the plasma plate power is adjusted from 21.1 kW to 27.2 kW.

2.3.2   Powder feeding rate

Powder feeding rate and the flow rate of carrier gas work together to change the speed of the powders and finally change the time of the powders' melting. With a higher speed, the melting time may not be sufficient so that the particles may not transform to liquid totally and the spheroidization ratio will be low. While, a slower speed may give rise to more evaporation of the TC4 alloy powders, causing the creation of nanometer powders absorbed to the spheroidized particles due to Van de Waals force during cooling process. And this will result in adhesions of different particles or a rougher surface. Comparing the spheroidization ratio of No.2, No.3 and No.4
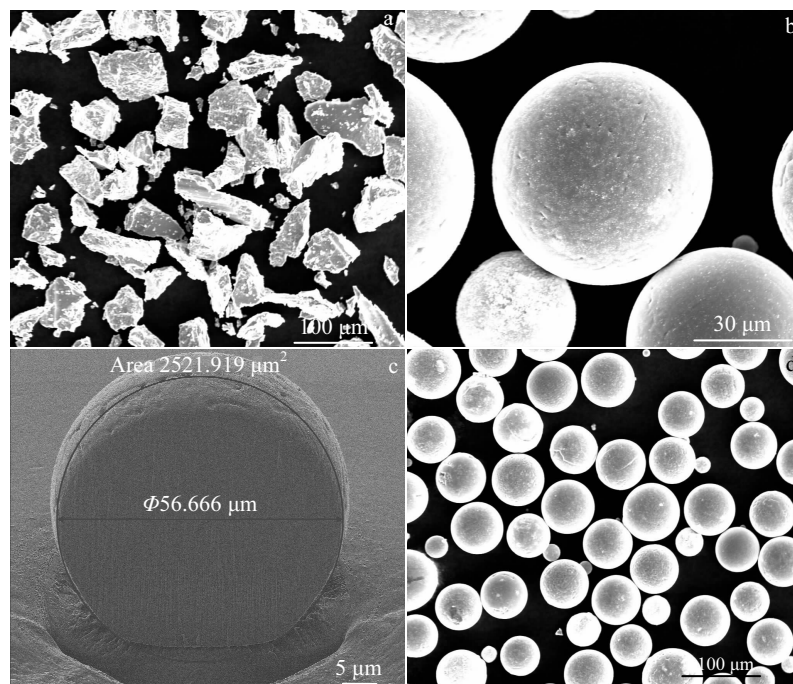

Fig.3   SEM images of TC4 alloy raw material powders (a) and corresponding spheroidizing powders (b), internal micro-structure (c), and surface morphology of the spheroidized particles (d)
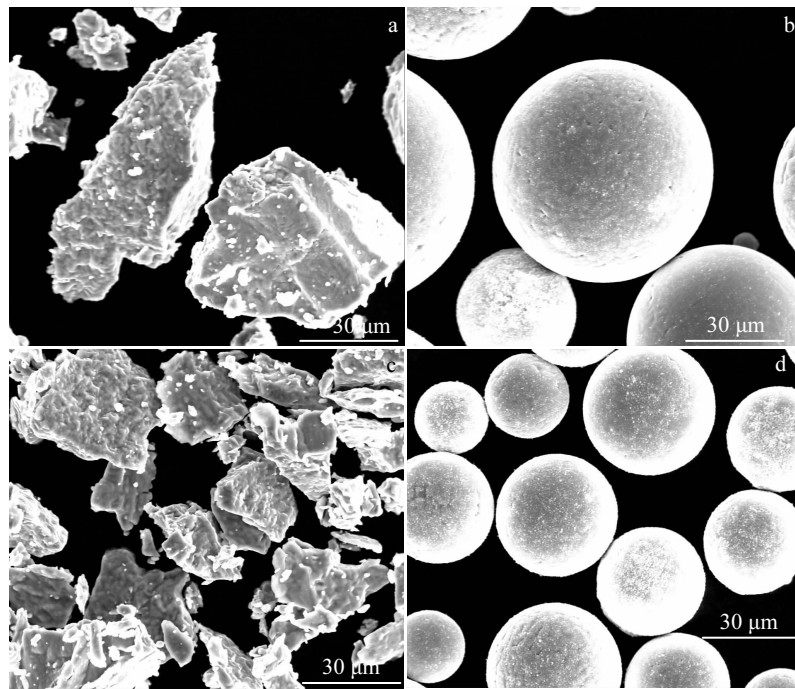
Fig.4   SEM images of TC4 alloy raw material powder with an average size of larger (a) or less than 38 μm (c), and the corresponding spheroidized powder (b) or (d)

Table 2   Spheroidization ratio under different contributory factors

No.	Particle size distribution/μm	Position of the inlet nozzle/cm	Chamber pressure/kPa	Powder feeding rate/g·min^{-1}	Plasma plate power/kW	Spheroidization ratio/%
1	<80	11.7	101.36	1.742	27.2	61.5
2	<80	12.5	101.36	1.742	27.2	96.4
3	<80	12.5	101.36	16.089	27.2	93.2
4	<80	12.5	101.36	0.908	27.2	88.4
5	<80	12.5	89.64	1.742	27.2	93.3
6	<80	12.5	68.95	1.742	27.2	91.9
7	<80	12.5	101.36	1.742	23.0	93.5
8	<80	12.5	101.36	1.742	21.1	77.1
9	38~63	12.5	101.36	1.742	27.2	98.5
10	38~63	12.0	101.36	1.742	27.2	98.4
11	38~63	11.5	101.36	1.742	27.2	98.4

in Table 2, one can find that 1.742 g/min is the best choice for this procedure. A higher rate or a slower rate will lead to a lower spheroidization ratio.

2.3.3   Chamber pressure

Chamber pressure is a complicated factor in the spheroidizing process, and it works together with the flow rate of the central gas to change the velocity distributions of the plasma. With a higher flow rate of the central gas and a lower chamber pressure, the plasma plume will have a higher speed implying a shorter dwell time for TC4 alloy particles; as a result, particles are melted incompletely and the spheroidization ratio is reduced inevitably. Therefore, for a higher spheroidization ratio, the chamber pressure should be

adjusted to a higher degree to slow down the flow rate of the thermal plasma. It can be seen from experiments No. 2, 5 and 6 that a higher chamber pressure makes a higher spheroidization ratio, which confirms the above judgement.

2.3.4   Particle size distribution

Particles with different diameters ask for different heat energy to melt totally, so particle size distribution has a direct influence on the spheroidization ratio. In comparison, particles with a narrower size distribution will have a higher spheroidization ratio because particles with a larger average diameter are hard to be melted totally which means more heat energy and a higher temperature of the plasma. But if the average diameter of the particles is so small, the powders will generate

agglomeration and have worse dispersibility. In this experiment, raw materials before sifting have a wide size distribution of around 20~80 μm which we can know from the product descriptions and the SEM images. After sifting with two screen meshes whose sizes are 400 eye and 240 eye we got particles with a narrower size distribution of around 38~63 μm. Test results of the particle size distribution after sifting are shown in Fig.5 which also proves that the size of the treated powders is in control in this process as we can see from the SEM images. We can compare No.2 with No.9 in Table 2, and find that the spheroidization ratio is 96.4% before sifting which is 2% less than that after sifting.

2.3.5 Position of the inlet nozzle

The position of the inlet nozzle determines the starting position of the powders when they are injected in the plasma plume. Here we use "z" marked in Fig. 1 to represent the position of the inlet nozzle. The instruction book indicates that with z=12.975 cm the starting position of the injected particles is just located at the middle of the induction coil, where the temperature is the highest. While, considering the fact that TC4 alloy powders feature a relatively lower density, a value of z less than 12.975 cm was chosen to avoid the TC4 alloy particles knocking at the quartz or ceramic tube around the plasma plump. Because quartz or ceramic tubes with TC4 alloy powders attached to them easily fracture, a series of inlet nozzle position of 12.5, 12.0, 11.7, and 11.5 cm were selected to prevent that destruction. For raw TC4 alloy powders without sifting, as the inlet nozzle position changes from 11.7 cm to 12.5 cm, the spheroidization ratio increases by about 34.9%, as shown with samples Nos. 1 and 2 in Table 2. While, in the case of sifting powders with size of 38~63 μm, the inlet nozzle position has no effect on the spheroidization ratio, which is demonstrated by samples Nos. 9, 10 and 11 in Table 2. Here, some qualitative calculations were conducted to explain the difference by using following equations[5,10]:

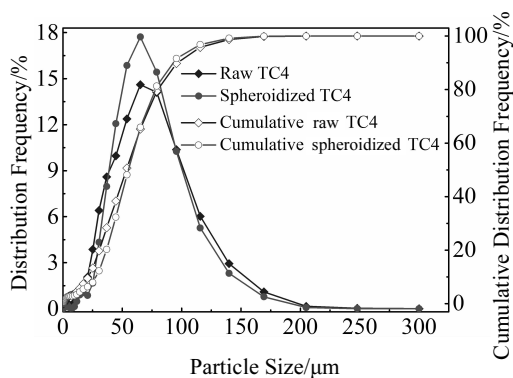$$t_h = \frac{\rho_p}{3} r_w^2 \int_{T_0}^{T_m} \frac{C_p \mathrm{d}T_p}{S_\infty - S_w} \tag{1}$$

$$S = \int_{T_0}^{T} k(T)\mathrm{d}T \tag{2}$$

$$t_m = \frac{r_w^2 \rho_v L_m}{3(S_\infty - S_m)} \tag{3}$$

where, in Eq.(1), t_h means heating time, T_0 is the starting temperature, T_m is the melting point, r_w, ρ_p, C_p mean the radii, density and heat capacity of particles, respectively. S_∞ and S_W represent the thermal conduction potential of the surrounding gases at plasma temperature and particle surface and can be calculated with Eq.(2), where k represents the thermal conductivity of plasma gas. The time of melting (t_m) for the particle of defined diameter (r_w) can be calculated by Eq.(3), where L_m is the heat of fusion of TC4 alloy powders and S_m is the thermal conductivity potential of plasma at the melting point. For calculation, values of L_m, C_p, and $k(T)$ were taken from Refs. [11-13]. The values of r_w, ρ_p, T_0 and T_m were 25 μm, 4.5 g/cm^3, 300 K and 1933 K, respectively. Therefore, t_m and t_h were estimated to be 0.49 ms and 1.36 ms, respectively. And, the whole melting time for powders totally melting is 1.85 ms. Particles flying in the plasma plume were assumed to have the same mean speed as the central gas. We roughly calculated the mean speed to be 5 m/s, and the length of plasma plume down to 2000 K along the central line was about 0.4 m[14]. Thereafter, the time for heating powders in the plasma plume is about 80 ms, which is enough for total melting.

While, the spheroidization ratio was not 100% and SEM images showed the un-melted particles generally had a larger average diameter. There were two reasons for these results. On the one hand, the position of the inlet nozzle is much lower than that we assumed. As a result, the length of plasma plume is much shorter resulting in a shorter time for powders flying and melting in the plume, leading to the insufficiently melted particles, especially for lager particles bigger than 25 μm. On the other hand, particles did not fly down along the central of the coil. The heating zone away from the center of the plasma plume had a lower temperature; besides, the plasma system and temperature distribution were not so stable [14]. So, when particles went through the low-temperature zone at the edge of the plasma plume, the particles especially bigger than 25 μm most likely could not be melted totally. Also, these two situations could explain the above differences in spheroidization ratio based on sifting raw powders with or without treatment. Large particles in un-sifted powders could be melted totally by adjusting the inlet position, and the spheroidization ratio was improved. After the treatment of sifting, size distribution of particles was more homogeneous without larger particles, and the inlet position was not so influential. Besides, after sifting, particles were separated one by one and the adhesion between them became weak, being good for absorbing more heat to melt totally.

2.4 Properties of the spherical powders

The fluidity of powders before and after spheroidizing process was measured. And the spheroidized powders show a

Fig.5 Particle size distribution of the raw materials and the treated powders

Table 3　Fluidity and bulk density of powders before and after the plasma treatment

Property	Before treatment	After treatment
Fluidity/s·(50 g)$^{-1}$	No fluidity	35.5
Bulk density/g·cm^{-3}	1.2153	2.2898

much better fluidity than raw TC4 alloy powders, as shown in Table 3. That is to say, the spheroidized powders have a natural fluidity of 35.5 s/50g, while the raw TC4 alloy powders just could not fall through the discharge port of the stainless funnel even with knocking the edge of the funnel. Moreover, after the spheroidizing process, the bulk density of the TC4 alloy powders was increased, which is good for the following practical use in industry.

3　Conclusions

1) Using a radio frequency plasma system, we can prepare spherical TC4 alloy powders with a spheroidization ratio being as high as 99% by combining raw powders with size of 38~63 μm with proper experimental parameters, such as, the inlet nozzle position of 12.5 cm, the chamber pressure of 101.36 kPa, the powder feeding rate of 1.742 g/min, and the plasma plate power of 27.2 kW.

2) The phase structure doesn't change after the plasma treatment. The spherical TC4 alloy powders are demonstrated to be filled and dense with relatively smooth surfaces.

Fluidity and bulk density are both higher than those of raw materials.

References

1　Filice L, Gagliardi F, Lazzaro S *et al*. *Amer Inst Physics*[J], 2011, 165:165

2　Temmler A, Walochnik M A, Willenborg E *et al*. *J Laser Appl*[J], 2015, 27(2): 1938

3　Yang J, Sun S, Brandt M *et al*. *J Mater Process Technol*[J], 2010, 210(11): 2215

4　Lemu H G. *AIP Conference*[J], 2012, 857(4): 857

5　Li Ya-Li, Ishigaki T. *J Am Chem Soc*[J], 2001, 84(9): 1929

6　Kumar S, Selvarajan V, Padmanabhan P V A *et al*. *J Mater Process Technol*[J], 2006, 176(2): 87

7　Sanon A, Baronnet J M. *IOP Conf Ser: Mater Sci Eng*[J], 2012, 29 (2): 12 003

8　Bonizzoni G, Vassallo E. *Vacuum*[J], 2002, 64(1): 327

9　Evans J L. *Eng Fail Anal*[J], 2010, 17(4): 882

10　Chen X, Pfender E. *Plasma Chem Plasma P*[J], 1982, 2(9): 293

11　Kumar C, Das M, Biswas P. *Lasers Based Manufacturing*[J], 2015(9): 421

12　Pateyron B, Elchinger M F, Delluc G *et al*. *Plasma Chem Plasma P*[J], 1992, 12(12): 421

13　Alderson N A. *Thesis for Doctorate*[D]. Raleigh: North Carolina State University, 2012

14　Chen K, Boulos M I. *J Phy D: Appl Phys*[J], 1994, 27(5): 946

射频等离子体法制备球形化 TC4 (Ti6Al4V)合金粉末

赵　翀，麻朝阳，文子诚，曹永革，马　冉，袁轩一

(中国人民大学 光电功能材料与微纳器件北京市重点实验室，北京　100872)

摘　要：采用射频等离子体法制备了高度球形化的 TC4(Ti6Al4V)合金粉末。主要探究仪器送粉喷嘴高度、产生等离子体的功率、反应室的压力、原料粉体的粒度分布、送粉速率以及载气的气流速率等对于粉体球化率的影响。通过 SEM 图像观察粉体的形貌变化并计算粉体的球化率，利用 XRD 图谱测定球化前后粉体相结构。结果表明，通过观察球化粉末横截面可知粉末为实心球体且表面光滑，球化后粉末流动性明显提高，松装密度增大，粒度分布变窄，适合 3D 打印等应用技术对于合金粉体的要求。实验中，调节送粉喷嘴高度为 12.5 cm，反应室压力为 101.36 kPa，送粉速率为 1.742 g/min，产生等离子气的功率为 27.2 kW 且控制原料粉体的粒度分布在 38~63 μm 时，可使得球化率达到 99%，明显高于其他球化粉末制备方法。

关键词：球化；Ti6Al4V 分粉体；射频等离子体

作者简介：赵　翀，女，1994 年生，博士生，中国人民大学光电功能材料与微纳器件北京市重点实验室，北京　100872，电话：0086-10-82502773，E-mail: 943381321@ruc.edu.cn